Electronic Supplementary Information

Skin-inspired Gradient Ionogels Induced by Electric Field for Ultrasensitive and Ultrafast-responsive Multifunctional Ionotronics

Min Xu,[a] Xuchao Shen,[b] Shuaijie Li,[a] Hongnan Zhu,[a] Yan Cheng,[a] Hongying Lv,[a] Zhuoer Wang,[a] Cunguang Lou,[b,*] and Hongzan Song,[a,*]

[a] College of Chemistry and Materials Science, Hebei University, Baoding, Hebei Province, 071002, P. R. China
[b] College of Electronic Information Engineering, Hebei University, Baoding, Hebei Province, 071002, P. R. China

***Corresponding Authors**

E-mails: loucunguang@163.com (C. LOU); songhongzan@iccas.ac.cn (H. Song).

1. Experimental section

1.1. Materials.

1-Butyl-3-methylimidazolium tetrafluoroborate ($BMIMBF_4$, 99%), 1-vinyl-3-butylimidazolium tetrafluoroborate ($VBIMBF_4$, 99%), 1-Butyl-3-methylimidazolium hexafluorophosphate ($BMIMPF_6$, 99%) and 1-vinyl-3-butylimidazolium hexafluorophosphate ($VBIMPF_6$, 99%) were purchased from Shanghai Cheng Jie Chemical Co. LTD. Ethyl phenyl(2,4,6-trimethylbenzoyl) phosphinate (98%) was purchased from Aladdin (Shanghai, China) and used without further purification. Acrylate-terminated hyperbranched polymer (HP) (Mn =2200 g/mol, with eight double bonds at the chain extremities on each molecule) was synthesized on the basis of our previous work.[1, 2] The molecular weight of HP was measured to be 2200 g/mol from GPC measurement.

1.2. Preparation of precursor solution.

The homogeneous and transparent precursor solution was prepared by adding an amount of $BMIMBF_4$ (solvent), $VBIMBF_4$ (monomer), HP (Macro-crosslinker), and Ethyl phenyl(2,4,6-trimethylbenzoyl) phosphinate (initiator) in a 20 mL glass bottle and stirred for 1h at 25 ^{o}C.

1.3 In-situ synthesis of gradient ionogels under electric field.

The above solution was dropped into the prepared ITO conductive glass mold, and the voltage of the DC power supply is adjusted to 3v to apply a stable electric field. After a suitable time of electrification, the above solution was polymerized under a UV chamber (8W, wavelength of 365 nm), and the gradient ionogel was obtained. The samples of other ionogels were prepared using the same method.

1.4. Characterization.

FTIR spectra were recorded on a spectrophotometer (Varian-640). Ultraviolet-visible spectrophotometer (WFZ UV-2000) was used to measure the transmittance of ionogel. The microstructure of ionogel was observed by scanning electron microscope (SEM) on a JEOL SEM 6700 operating at 10 kV. The glass transition temperature (Tg) of ionogel was measured by a differential scanning calorimeter (DSC Q8000, TA Instruments). The thermal stability of ionogel was tested by a Thermogravimetric analyzer (Pyris6, PerkinElmer). The Rheological measurements were performed on MCR-702 rheometer (Anton Paar Company, Austria) with 8 mm parallel-plate geometry at 25 °C. The tensile properties of ionogels were tested on Linkam TST 350 tensile hot stage (Linkham, UK) and Universal testing machine (WDW-02). The compression properties were tested by a stress-controlled rheometer (TA-AR2000EX, TA Instruments). The electrochemical performance of ionogel was measured by the Ivium electrochemical workstation (V01330, IVIUM Technologies BV). Ionic conductivity was calculated from the bulk resistances obtained from the impedance spectra ($\sigma = d/(RS)$). The sensor performance was measured by the Keithley DMM7510 system electrometer. Statement: This study is conducted in accordance with The Code of Ethics of the World Medical Association (Declaration of Helsinki). Two authors (Min Xu and Shuaijie Li) have given their informed consent for participation in the research study. All experiments have performed in compliance with the relevant guidelines. The study protocol and the informed consent form were both approved by Ethics Committee of Affiliated Hospital of Hebei University.

References:

1. *K. Zhao, H. Song, X. Duan, Z. Wang, J. Liu and X. Ba. Polymers, 2019, 11, 444.*
2. *Z. Wang, J. Zhang, J. Liu, S. Hao, H. Song and J. Zhang, ACS App. Mater. Interfaces, 2021, 13, 5614-5624.*

2. Supplementary table.

Table S1 Composition of the ionogels

Samples	PIL/*wt*%	IL/*wt*%	HP in PIL/*wt*%
25%-Ionogel	**25**	**75**	**1**
30%-Ionogel	**30**	**70**	**1**
35%-Ionogel	**35**	**65**	**1**

Table S2. Comparison between this work and previously reported iontronic sensors.

Sensitivity	Response time	Temperature range	Detection range	Refs.
1.0 kPa^{-1}	8 ms	-85-360 °C	0.15 Pa-0.4 MPa	This work
0.04 kPa^{-1}	-	-	10 Pa-1 MPa	ACS Materials Lett. 2022, 4, 2459
0.51 kPa^{-1}	100 ms	-	10 Pa-1 MPa	J. Mater. Chem. A, 2023, 11, 7201–7212
5.93×10^{-3} Pa^{-1}	200 ms	-40-283 °C	1 kPa-0.1 MPa	Adv. Mater. 2021, 33, 2105306
1.62nF/kPa	8 ms	-108-300 °C	300 Pa-2.5 MPa	Adv. Mater. 2021, 33, 2008486
0.05 kPa^{-1}	150 ms	-	0-6.67 kPa	Adv. Funct. Mater. 2018, 28, 1802576
0.91 kPa^{-1}	40 ms	-	63 Pa-88 KPa	Mater. Horiz., 2022, 9, 1935-1946
0.04 kPa^{-1}	-	10-90 °C	0-8.29 kPa	Nat. Commun. 2018, 9, 1134
0.023 kPa^{-1}	-	-72 °C -	0-3.23 MPa	Chem. Eng. J., 2021, 403, 126431
	15-100 ms	0.6-48 °C	1 kPa-1 MPa	Human skin

3. Supplementary pictures.

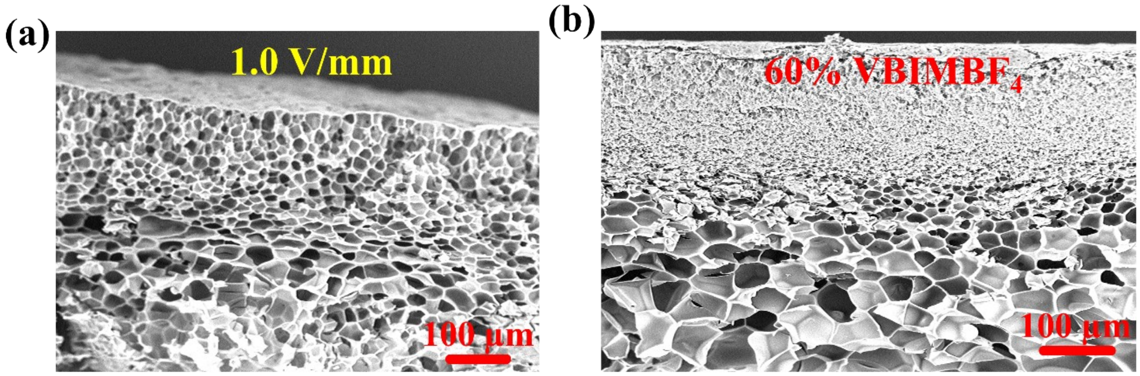

Fig. S1. (a) SEM images of the ionogel prepared under voltage 1.0 V/mm. (b) SEM images of the ionogel with 60% $VBIMBF_4$.

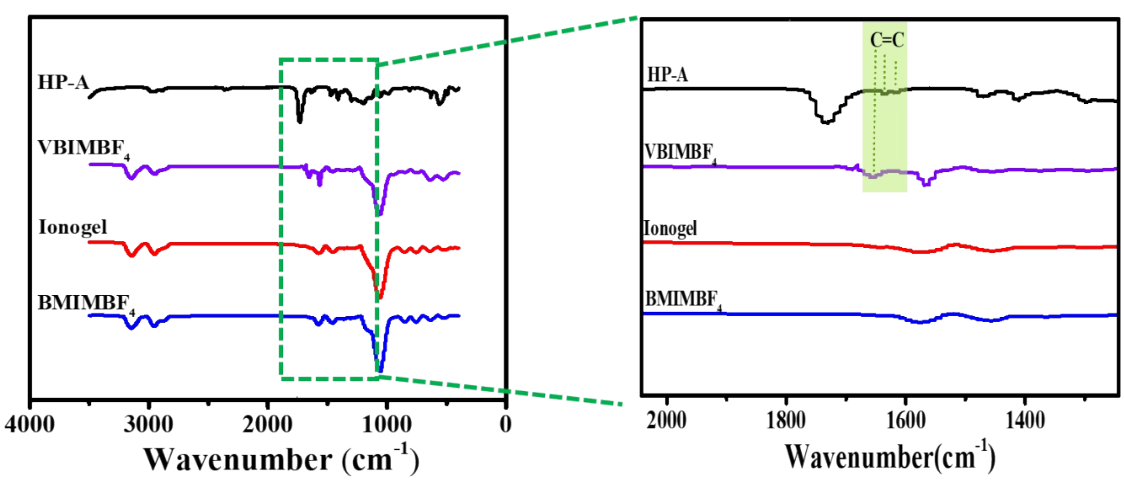

Fig. S2. FTIR patterns of $BMIMBF_4$, VBIMBF4, HP-A, and ionogel.

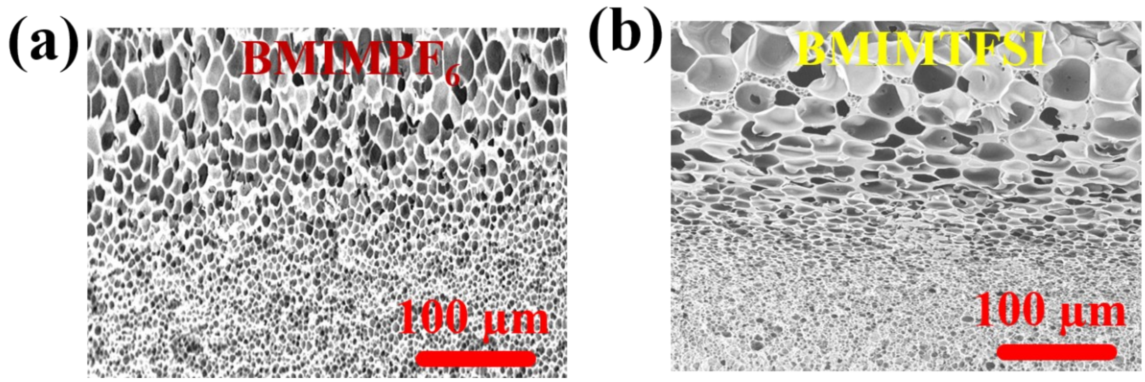

Fig. S3. (a) SEM images of Poly(VBIMPF$_6$)/BMIMPF$_6$ ionogel. (b) SEM images of Poly(VBIMTFSI)/BMIMTFSI ionogel.

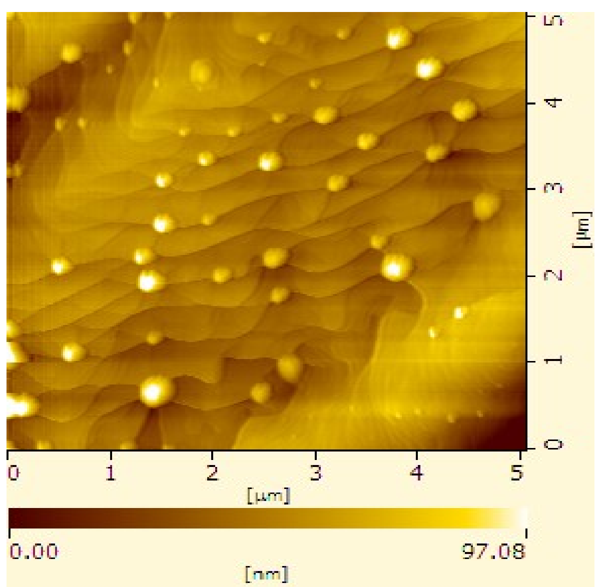

Fig. S4. AFM image showing homogenous dispersed the nano-sized macro-cross-linker of HP.

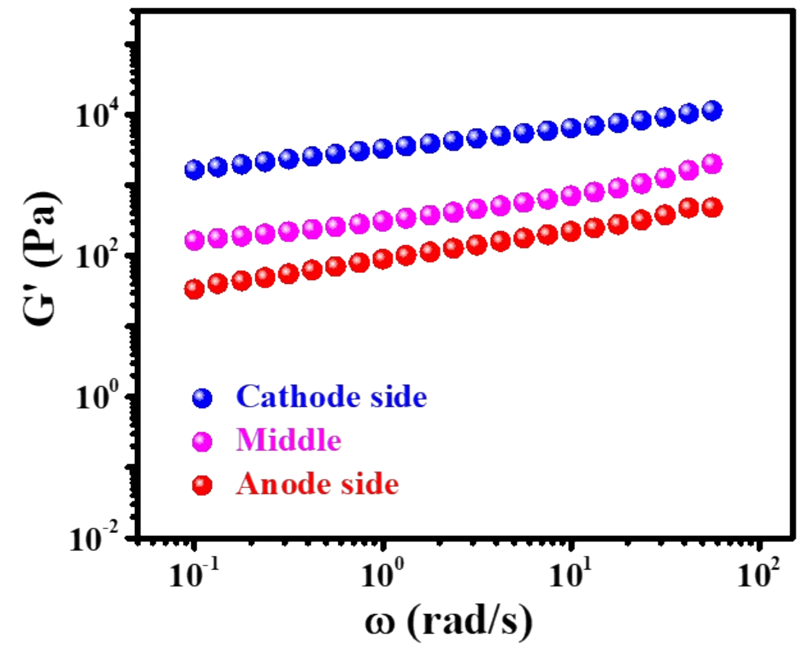

Fig. S5. The frequency sweeping curves at the cathode side, middle, and the anode side.

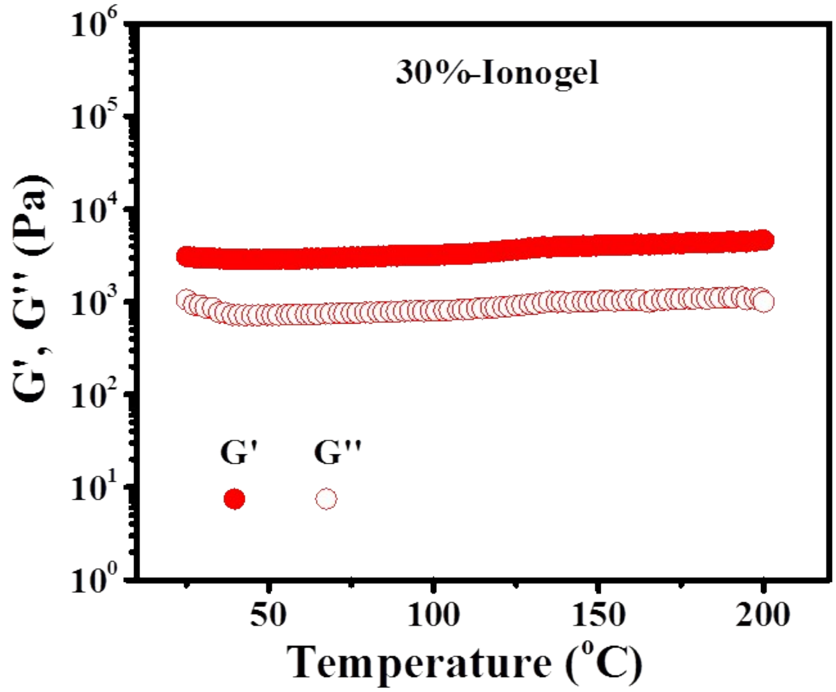

Fig. S6. Changes of G′ and G″ with increasing temperature from 25 to 200 ^{o}C.

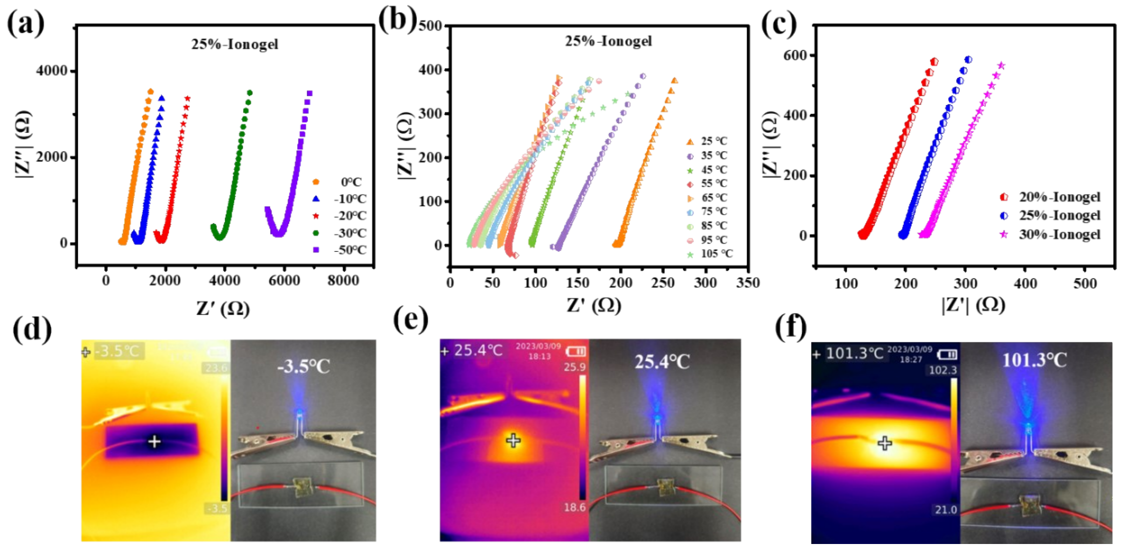

Fig. S7. (a)-(b) Impedance plots of 25%-Ionogel under different temperature. (c) Impedance plots of ionogels with different content of PIL. (d)-(f) Photographs of the change in the LED lightness under different temperature.

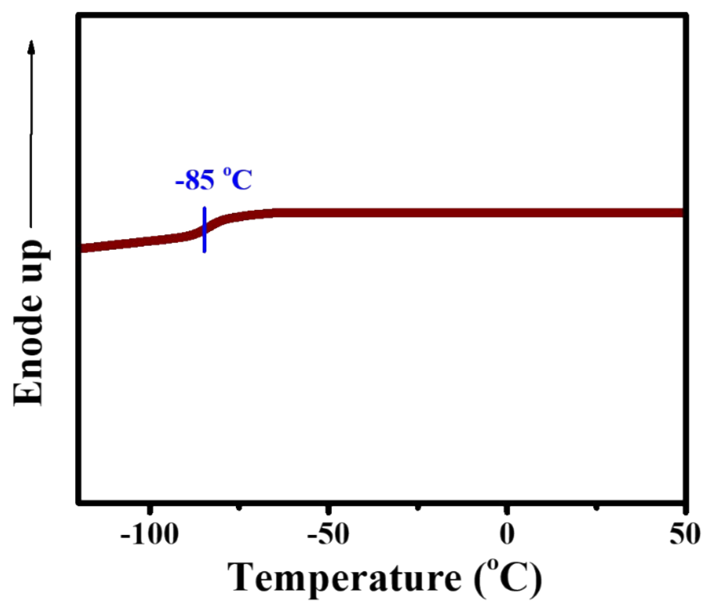

Fig. S8. DSC curve of the gradient 25%-Ionogel between -120 and 50 °C.

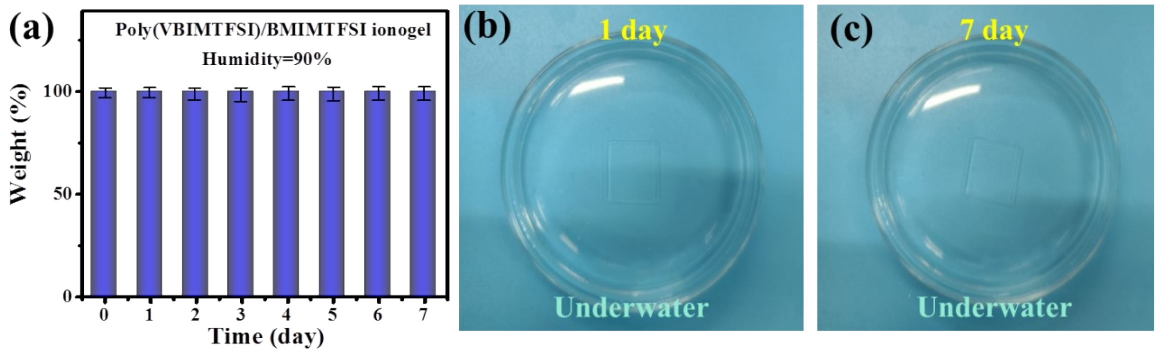

Fig. S9. (a) The stability of the ionogels at a relative humidity of 90% for different time. (b) and (c) The photographs of the sample in water for 1 and 7 day.

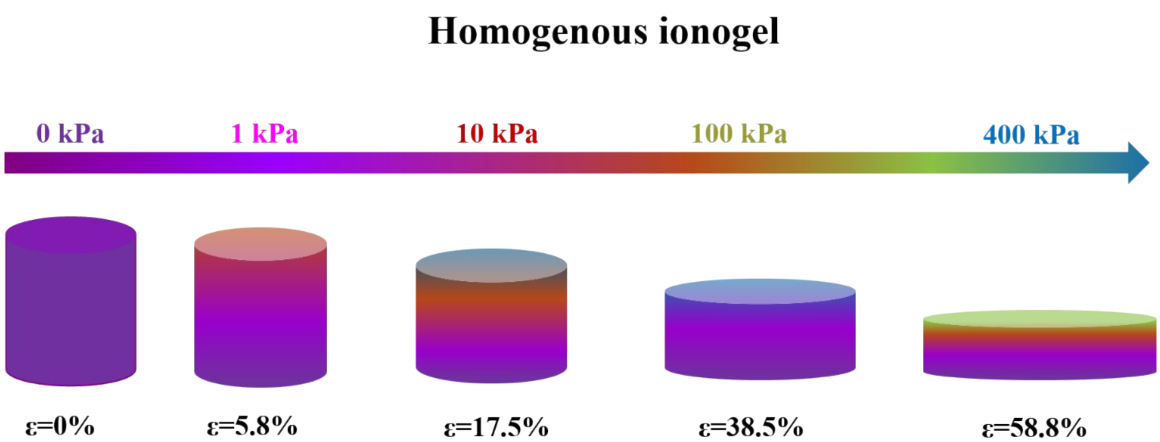

Fig. S10. The simulation diagram of homogenous ionogels under different stresses via finite element method with ANSYS software.

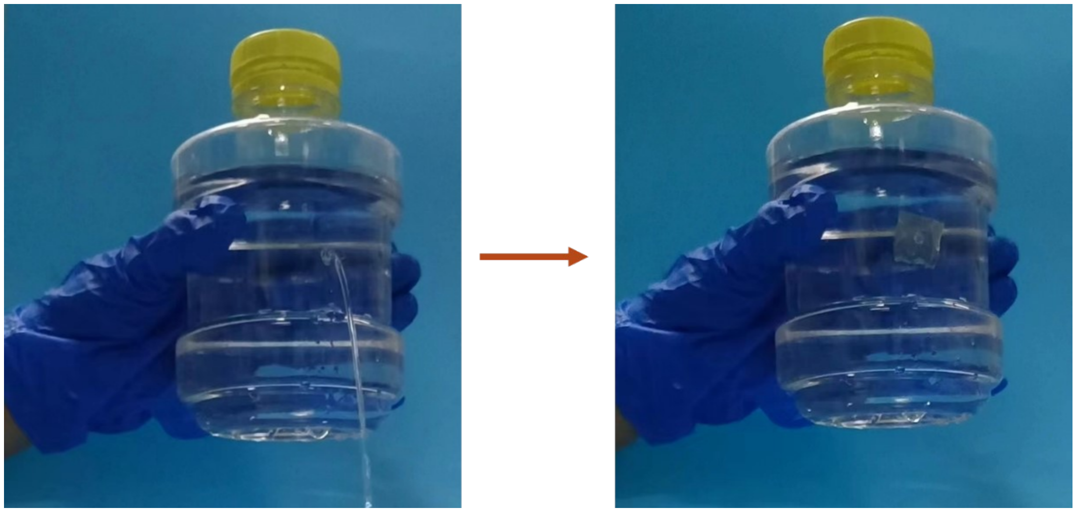

Fig. S11. The photographs demonstrate the hydrophobic ionogel with good adhesive property.

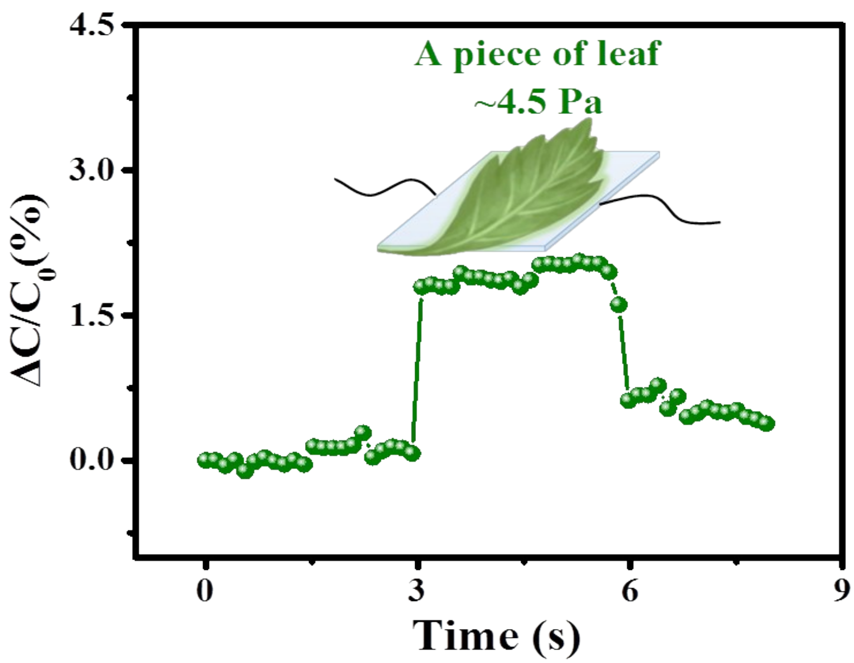

Fig. S12. Detection of small object (a piece of leaf) about 4.5 Pa.

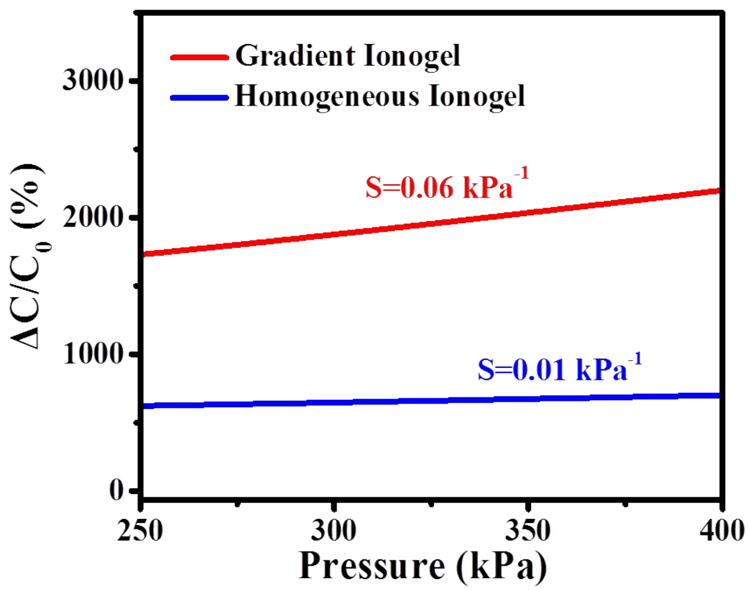

Fig. S13. Relative change of $\Delta C/C_0$ versus pressure in the high-pressure region (250-400 kPa).

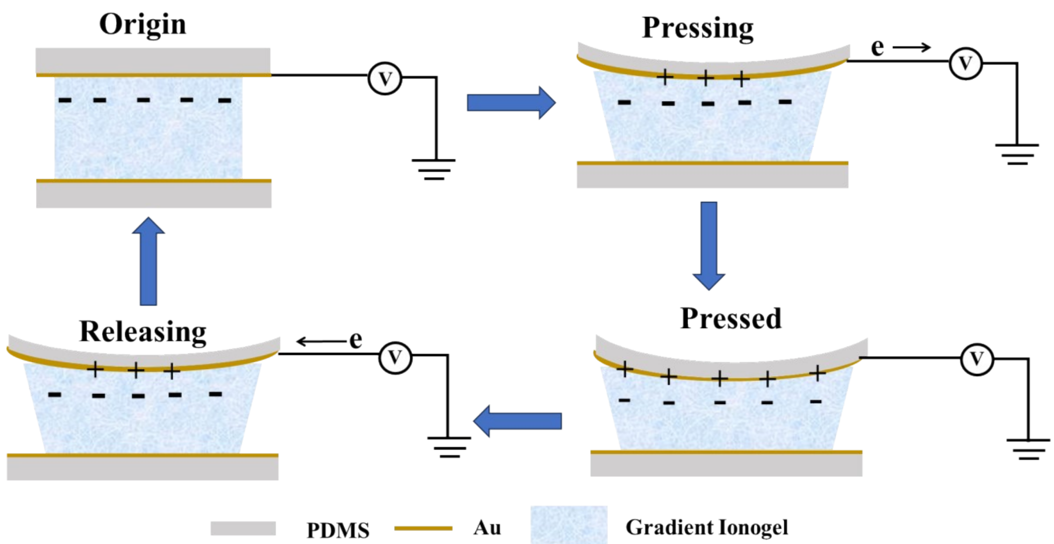

Fig. S14. Diagrams of the working mechanism of the sensor. The triboelectric charges are driving back-and-forth between the Au electrode and ground as the ionogel being pressed and released.